Nic1 Inactivation Enables Stable Isotope Labeling with $^{13}C_6{}^{15}N_4$-Arginine in *Schizosaccharomyces pombe**

Alejandro Carpy‡¶, Avinash Patel§¶, Ye Dee Tay§, Iain M. Hagan§, and Boris Macek‡‖

Stable Isotope Labeling by Amino Acids (SILAC) is a commonly used method in quantitative proteomics. Because of compatibility with trypsin digestion, arginine and lysine are the most widely used amino acids for SILAC labeling. We observed that *Schizosaccharomyces pombe* (fission yeast) cannot be labeled with a specific form of arginine, $^{13}C_6{}^{15}N_4$-arginine (Arg-10), which limits the exploitation of SILAC technology in this model organism. We hypothesized that in the fission yeast the guanidinium group of $^{13}C_6{}^{15}N_4$-arginine is catabolized by arginase and urease activity to $^{15}N_1$-labeled ammonia that is used as a precursor for general amino acid biosynthesis. We show that disruption of Ni^{2+}-dependent urease activity, through deletion of the sole Ni^{2+} transporter Nic1, blocks this recycling in ammonium-supplemented EMMG medium to enable $^{13}C_6{}^{15}N_4$-arginine labeling for SILAC strategies in *S. pombe*. Finally, we employed Arg-10 in a triple-SILAC experiment to perform quantitative comparison of G1 + S, M, and G2 cell cycle phases in *S. pombe*. *Molecular & Cellular Proteomics 14: 10.1074/mcp.O114.045302, 243–250, 2015.*

Stable Isotope Labeling by Amino acids in Cell culture (SILAC)[1] is one of the most widely used methods in quantitative proteomics (1). It involves *in vivo* metabolic labeling of cell cultures (or small organisms) with different versions of stable isotope-labeled amino acids (2). To maximize the number of peptides that can be quantified after proteome digestion with trypsin, proteins are usually differentially labeled with different forms of lysine and arginine (3): L-lysine (Lys-0) and L-arginine (Arg-0); $^{2}H_4$-lysine(Lys-4) and $^{13}C_6$-arginine (Arg-6); or $^{13}C_6$-$^{15}N_2$-lysine (Lys-8) and $^{13}C_6$-$^{15}N_4$-arginine (Arg-10). The availability of multiple forms of labeled lysine and arginine support the application of SILAC in duplex (comparison of two states) or triplex (comparison of three states) formats. Efficient anabolic pathways mean that lysine and arginine are not essential for growth of wild type yeast cells. Auxotrophic mutants that are defective in these pathways can be used to switch yeast to an absolute dependence upon the provision of these amino acids in the external medium. Consequently, mutations in arginine and lysine biosynthesis pathways can be used to drive the complete labeling of all tryptic peptides with specific forms of these amino acids (4, 5). SILAC has been used in quantitative proteomics in several yeast species, but most widely in *Saccharomyces cerevisiae* (6) (budding yeast) and *Schizosaccharomyces pombe* (fission yeast). *S. pombe* is extensively exploited to study cell cycle control (7), heterochromatin (8), and differentiation (9) and is increasingly the subject of large-scale quantitative proteomic studies (10, 11).

A major challenge that is faced when using SILAC in fission yeast, is metabolic conversion of arginine to other amino acids such as proline, glutamine, and lysine (5). This partial labeling of additional amino acids after the conversion event produces spectra with complex isotope clusters that makes the downstream analysis challenging and error-prone. Inactivation of the "arginine conversion pathway" by removal of the orthinine transferase, Car2, effectively overcomes this problem to support the use of arginine labeling in SILAC-based experiments (5). Although this exploitation of the *car2.*Δ mutation now enables SILAC technology in fission yeast, the choice of amino acids that can be employed remains limited. Only one form of heavy arginine (R6) is currently used alongside three forms of heavy lysine (Lys-4, Lys-6, and Lys-8) (5, 12). Surprisingly, we could not find any studies that use arginine (Arg-10) in fission yeast, even though this is a widely exploited reagent for labeling other cell types (1).

Here, we show that labeling of fission yeast with Arg-10 leads to a general misincorporation of the stable isotope label that prevents the identification of labeled peptides. We hypothesize that successive arginase and urease activities catabolize the guanidinium group of Arg-10 to $^{15}N_1$-labeled ammonia. This labeled ammonium is then used as a general

From the ‡Proteome Center Tuebingen, University of Tuebingen, Tuebingen, 72076, Germany; §CRUK Cell Division Group, CRUK Manchester Research Institute, University of Manchester, Manchester, M20 4BX, UK

⌘ *Author's Choice*—Final version full access.

Received, September 30, 2014 and in revised form, November 3, 2014

Published, MCP Papers in Press, November 3, 2014, DOI 10.1074/mcp.O114.045302

Author contributions: I.M.H. and B.M. designed research; A.C., A.P., and Y.D.T. performed research; A.C. and Y.D.T. analyzed data; A.C., I.M.H., and B.M. wrote the paper.

[1] The abbreviations used are: SILAC, stable isotope labeling by amino acids in cell culture; YES, solid yeast extract agar; EMM, Edinburgh minimal media.

precursor for amino acid biosynthesis. Disruption of Ni^{2+}-dependent urease activity through deletion of Ni^{2+} transporter Nic1 in ammonium-supplemented medium, blocked this recycling to support $^{13}C_6{}^{15}N_4$-arginine labeling SILAC strategies. As a proof of principle we employ Arg-10 in a triple-SILAC experiment to perform quantitative comparison of G1 + S, M, and G2 cell cycle phases in *S. pombe*.

EXPERIMENTAL PROCEDURES

Yeast Strains—

Standard Yeast Culture—Strains used in this used study are listed Table 1. Cell culture and maintenance were according to Moreno *et al.* (13). The amino acid supplements were uracil, adenine, leucine, and histidine at a concentration of 200 μg/ml. Yeast strains were streaked onto YES plates (Solid Yeast Extract agar with supplements) from frozen glycerol stocks at −80 °C, and grown at the permissive temperature (25 °C) until single colonies formed. One single colony was used to start each liquid culture. For all physiological experiments, asynchronous cultures of cells were grown in variants of Edinburgh minimal media 2 (EMM2), with appropriate supplements from log phase starter cultures ($1 \times 10^6 - 5 \times 10^6$ cells/ml). In EMMG, the 5g/L ammonium chloride of EMM2 is replaced with 5g/L monosodium glutamate (14). In EMMGn, EMMG is supplemented with 12 mM NH_4Cl.

S. pombe Transformation Using Lithium Acetate—Cultures that had been grown in YES (nutrient rich) to mid-log phase ($4 \times 10^6 - 8 \times 10^6$ cells/ml) were pelleted by centrifugation at 3400 × *g* for 2 min, washed once in water followed by resuspension in appropriate volume of lithium acetate (0.1 M, pH 4.9) to a final density of 2×10^8 cells/ml. After 1 h at 25 °C 10–15 μg of DNA was added to 100 μl of competent cells alongside 2.9 volumes of PEG 4000 (50% (w/v) in 0.1 M, pH 4.9 lithium acetate). After 1 h at 25 °C and 15 min at 42 °C cells were washed once in water and plated onto selective minimal media.

SILAC-labeling—L-lysine:2HCl (4,4,5,5-D4, 96–98%, Cambridge Isotopes, cat no. DLM-2640–0.5) and L-arginine:HCl (U-13C6, 99%, Cambridge Isotopes, cat no. CLM-2265-H-0.5) were used as medium isotopic labels; L-lysine:2HCl (U-13C6, 99%; U-15N2, 99%, Cambridge Isotopes, cat no. CNLM-291-H-0.25), and L-arginine:HCl (U-13C6, 99%; U-15N4, 99%, Cambridge Isotopes, cat no. CNLM-539-H-0.5) were used as heavy isotopic labels.

Cell Culture—EMMG media is equivalent to EMM2 (15) except that 5 g/L ammonium chloride is replaced with 5 g/L monosodium glutamate (14). EMM2 media was also prepared with a range of ammonium chloride concentrations up to 96 mM. EMMGn is EMMG containing 12 mM NH_4Cl. To label the cells with heavy or medium isotopes of Arginine (R) and Lysine (K), starter cultures were prepared by inoculation into EMMG/EMMGn supplemented with 37.5 μg/ml each of light and medium/heavy isotopic versions of arginine and lysine. After inoculation from log phase starter cultures, main cultures were grown in EMMG/EMMGn supplemented with 75 μg/ml of heavy isotopic labeled R and K for at least 10 generations before sampling to ensure the maximum labeling of the proteome. Care was taken that the culture never grew beyond mid-log phase ($1 - 5 \times 10^6$). Each culture was harvested at mid-log phase. For direct comparisons with the EMM2 experiments of Bicho *et al.* (5) it was necessary to make starter cultures in YES media before inoculation into EMM2, as we were repeatedly unable to get growth in main cultures of either the *SILAC* strain when both the starter and main culture were made in minimal selective medium.

SILAC Strain—The 100 bp primer pair (CAR2_FORW, AAGTCAGATTATCAAAGGAGTTAAGAGATTATTGTGTAATCTTGAATCAGTTTTCTTTAGGTCTTAGTAAATTCTTCATTCGGATCCCCGGGTTAATTAA; CAR2_REV, TGTAGTCATCGAACCCTTAACATTAGAAGGGAGGTAAGTAAGAATGAATCGTCTAGTTTTTTTGTTTAAAGCATTGTTTTGAATTCGAGCTCGTTTAAAC) were designed such that the first 80 nucleotides were homologous to the sequences flanking the *car2*$^+$ gene and the last 20 nucleotides were homologous to the sequences of the pYM14 template plasmid that flanked the *natMX6* marker (*pFA6natMX6*) (16). The PCR product was transformed into the strain 5224 (*pku70::kanMX6 ura4.d18 leu1.32 ade6.704*). Emergent colonies that were resistant to Nourseothricin/ClonNat (Werner BioAgents, Jena, Germany, 96736–11-7) were selected. After PCR analysis confirmed the desired integration event, two rounds of back-crossing to wt removed *pku70::kanMX6* before arginine and lysine auxotrophic markers *arg3.D4* and *lys1.131 were* introduced to generate the *SILAC* strain (*car2::natMX6 arg3.D4 lys1.131*; IH 9091 and 9092).

SILACn Strain—The 100 bp primer pair (NIC1_FORW, AAAATTGTTATTATTATTGGAATCCTAAGTGGATACAGGTTTATGTGAACGCAATCTATTCAAATTACGCGTTTATTTGTTTAATTAAGGCGCGCCAGAT; NIC1_REV, ACGACTGGGAATTTCTGTTTCCTTTTTTTTTCTTCAGTATTCTCGATTTGTTCTCTTAACCTGTTGCTTGGGTTAAAAGTGTTTAAACTGGATGGCGGCG) were designed such that the first 80 nucleotides were homologous to the sequences flanking the *nic1*$^+$ gene and the last 20 nucleotides were homologous to the pYM14 template plasmid with the *natMX6* marker (*pFA6natMX6*) (5, 16). The PCR product was transformed into the strain IH6113 (*pku80::ura4*$^+$ *ura4.d18 leu1.32*). Emergent colonies that were resistant to Geneticin (MP Biomedicals, 158782) were selected. After PCR analysis confirmed the desired integration event, two rounds of back-crossing to wt preceded crossing into the *SILAC* base strain generated the *SILACn* base strain (*h- nic1::KanMX6 car2::NatMX6 lys1.131 arg3.D4*; IH 11849).

Cell Extracts for Proteomics Experiments—5×10^7 cells in log phase of growth were harvested at 4000 rpm for 2 min in screw cap 1.5 ml microfuge tubes. Cell pellets were washed once in ice-cold STOP buffer (10 mM EDTA, 50 mM NaF, 150 mM NaCl, and 1 mM NaN_3) before being flash frozen in liquid nitrogen and stored at −80 °C. Proteins were extracted by breaking the cells with 200 μl acid washed glass beads in the presence of 200 μl of denaturation buffer (6 M Urea, 2 M Thio-urea in 10 mM Tris buffer, pH 8.0) in a ribolyser (Fast prep FP120-BIO101, ThermoSavant, Carlsbad, CA) used for 30 s at 6.5 rpm. 200 μl of denaturation buffer was added to the glass beads before incubation on a rotating rocker at RT for 30 min. A hole was made in the bottom of each tube before each was placed on the top of an empty 1.5 ml microfuge tube and spun at 4800 rpm for 2 min at RT. The insoluble debris was separated by centrifugation at 13,000 rpm for 10 min at RT. The supernatant was collected in a fresh 1.5 ml microfuge tube to be processed for LC-MS/MS. Protein concentration was measured using Bradford reagent.

In-solution Protein Alkylation and Digestion—Reduction buffer [1 M dithiothreitol (DTT) in 50 mM ammonium bicarbonate (ABC)] was added to the sample to a final concentration of 1 mM DTT before a 1h incubation at room temperature (RT). After reduction, alkylation buffer [550 mM iodoacetamide (IAA) in 50 mM ABC] was added to a final concentration of 5.5 mM IAA before a further 1h incubation at RT in the dark. The sample was then digested with endopeptidase LysC (Wako Pure Chemical Industries, Japan, 1:100 enzyme:protein) at RT for 3 h. After digestion with LysC at high urea concentration, the sample was diluted to a final concentration of 1.2 M urea/0.4 M thiourea with MiliQ water and digested with trypsin (Promega, Fitchburg, MA, 1:100 enzyme:protein) at RT overnight. The samples were acidified to inactivate trypsin by adding 1% TFA or fractionated using Off-Gel isoelectric focusing as described below (17) and desalted using C18 StageTips (18).

Off-Gel Isoelectric Focusing—Off-Gel separation was performed as described by Krug *et al.* (17). Briefly, peptide samples were sep-

arated into 12 fractions using 13 cm Immobiline DryStrips with a pH 3–10 gradient (GE Healthcare) with the 3100 Off-Gel fractionator (Agilent, Santa Clara, CA). A maximum of 50 μA were applied until 20 kVH were reached. Peptide fractions were acidified with 10 μl of 30% ACN, 5% acetic acid, and 10% TFA in water.

MS Analysis—Desalted peptide fractions were separated using a nano-LC (Proxeon Biosystems) coupled to either an Orbitrap Elite or a LTQ Orbitrap XL (Thermo Fisher Scientific) mass spectrometer (MS). Peptides were separated on a 15 cm PicoTip fused silica emitter with a 75 μm ID (New Objective) packed, in-house, with ReproSil-Pur C18-AQ 3 μm resin (Dr. Maisch GmbH). Peptides were loaded on the column in Buffer A (0.5% acetic acid) at 700 nL/min using a maximum pressure of 280 Bar. Peptides were then eluted using a 57 or 87 min segmented gradient of 5–50% Buffer B (80% ACN in 0.5% acetic acid) at a flow rate of 200 nL/min. The mass spectrometers were operated in the positive ion mode. Spectra were recorded with data-dependent mode using a dynamic exclusion of 90 s (LTQ Orbitrap XL) or 60 s (Orbitrap Elite). Resolution was set at 60,000 (LTQ Orbitrap XL) or 120,000 (Orbitrap Elite) with an accumulation target value of 1E6 charges. For peptide analysis the 10 (LTQ Orbitrap XL) or 20 (Orbitrap Elite) most intense peaks were selected from the survey scan (300–2000 Thompson) and fragmented with collision induced dissociation at a target value of 5000 charges and recorded in the linear ion trap.

MS Data Processing—The MS data were analyzed with the MaxQuant Software Package version 1.3.0.5 (19) and searched using the Andromeda peptide search engine (20). The MS/MS spectra were searched against a database containing the proteome sequence of the *S. pombe* downloaded from PomBase (03.01.2013). The database contained 5145 entries from the *S. pombe* proteome, 248 frequently observed contaminants (downloaded from http://www.maxquant.org/contaminants.zip), as well as the reverse version of all sequences. Mass tolerance was set to 6 ppm at the MS and 0.5 Da at the MS/MS level. A minimal length of seven amino acids and full tryptic enzyme specificity were required. Two enzyme missed cleavages were allowed. Oxidation of methionine and protein N-terminal acetylation were defined as variable modifications and carbamidomethylation of cysteines was used as fixed modification. The false discovery rate was set to 1% on the peptide and protein level. In quantitative measurements, SILAC amino acids Lys4, Lys8, Arg6, and/or Arg10 were defined as fixed modifications. Significantly regulated protein groups were defined as those with calculated "Significance B" lower than 0.01.

Immunofluoresence and FACS Analysis—FACs analysis and Immunofluorescence microscopy were performed as described by Tay *et al.* (21). The Sad1 (spindle pole body component) and TAT1 (Trypanosome Alfa Tubulin) (22) primary antibodies were diluted 1:25 and 1:80 respectively. FITC anti-mouse antibody (Sigma Aldrich) and Cy3 anti-rabbit antibody (Sigma Aldrich) were used in PEMBAL as secondary antibodies for Sad1 and TAT1 at dilutions of 1:100 and 1:2500 respectively. Cytox green (Invitrogen, Carlsbad, CA) was used in FACS analysis.

RESULTS AND DISCUSSION

To assess the feasibility of using arginine (Arg-10) for quantitative proteomics of fission yeast, we performed SILAC labeling of *S. pombe* cells as described by Bicho *et al.* (5). We used *arg3.D4 lys3.131 car2::natMX6* background and refer to this genotype as *"SILAC"* in the following text. Consistent with previous observations (5), the *SILAC* strain grows poorly in the EMM2 medium that uses ammonium as a nitrogen source (Fig. 1*A*). Ammonium ions inhibit one of two arginine uptake pathways, to severely compromise the growth of arginine auxotrophs such as the *SILAC* strain (23). Substitution of ammonium for monosodium glutamate in the medium EMMG enables both arginine import pathways to be used. Mid-log phase growth of the *SILAC* strain in EMMG was comparable to wild type growth in the same medium (Fig. 1*A*, 1*B*). We therefore grew cells in EMMG rather than the reduced ammonium EMM2 used by Bicho *et al.* EMMG is widely used throughout the fission yeast community and, beyond an impact upon TOR growth controls (24), no differences from growth on EMM2 have been observed. However, as an additional check we asked whether the inclusion of the *SILAC* mutations affected the expression of mitotic phenotypes arising from incapacitation of both polo kinase and the kinesin 5 motor protein? Shifting a *plo1.ts41 cut7.24 SILAC* strain to 36 °C (25, 26) led to an efficient mitotic arrest, indicating that neither the switch of nitrogen source, nor the incorporation of *SILAC* mutations, had any impact upon the degree of mitotic arrest invoked by these mutations (Fig. 1*C*).

While performing a standard triple SILAC experiment using "light" (Lys-0 and Arg-0), "medium" (Lys-4 and Arg-6), and "heavy" (Lys-8 and Arg-10) amino acids in EMMG we noticed that almost all heavy (Lys-8 and Arg-10)-labeled peptides had complex isotope clusters that effectively prevented identification of heavy peptides and proteins. The presence both arginine- and lysine-containing peptides in these complex clusters (Fig. 2*A*) is indicative of a global conversion of the stable isotope label of either, the heavy arginine and/or lysine. To characterize the labeling problem in greater depth, we analyzed the light, medium-heavy, and heavy labeled samples separately. The identification rate for light and medium-heavy labeled samples was normal, whereas it was significantly reduced in samples from heavy labeled cells. To pinpoint the heavy amino acid responsible for the conversion, we measured samples labeled with a single heavy label (Arg-0/Lys-8 or Arg-10/Lys-0). Only the sample containing heavy arginine (Arg-10/Lys-0) presented the complex isotope clusters that reduced identification rates at both protein and peptide level. Thus, Arg-10 is incompatible with SILAC labeling approaches currently used for fission yeast analyses (Fig. 2*B*; a summary of the proteins identified in each experiment is presented in supplementary Tables S1 to S15).

We reasoned that this extensive mislabeling of multiple amino acids probably arose from catabolism of guanidine group of heavy arginine (Arg-10) to heavy urea. Catalysis by Car1 and Aru1 would convert the guanidine group into urea that could be further catabolized by ureases into ammonia (Fig. 1*D*) (5). The $^{15}N_1$-ammonia derived from $^{15}N_2$-urea would then be incorporated into multiple amino acids, each containing different numbers of ^{15}N atoms to alter the isotope distributions of all peptides. Unlike the medium-heavy $^{13}C_6$-arginine (Arg-6), only heavy $^{15}N_4{}^{13}C_6$-arginine (Arg-10) has isotopically labeled nitrogen and so only samples labeled with this form of arginine (Arg-10) are vulnerable to this urease catabolism problem. Consistently, conversion was not observed in measurements of

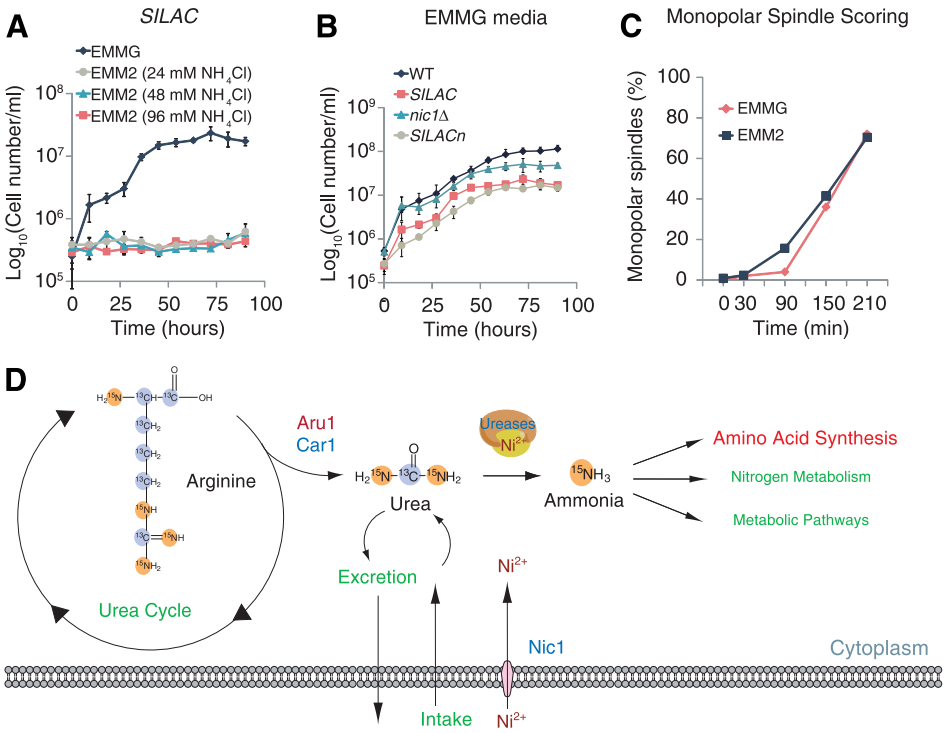

FIG. 1. **Metabolic characterization of *S. pombe*.** *A*, Growth curve of the *SILAC* strain in EMMG and EMMS media supplemented with different concentrations of ammonium chloride. *B*, Growth curve of WT, *SILAC, nic1*Δ, and *SILACn* strains in EMMG media at 25 °C. *C*, Scoring spindle formation defect in, *plo1.ts41 cut7.24 SILAC* cells during grown in the EMMG and EMMS media. Cultures were grown at 25 °C to a cell density of 1×10^6 before a shift to 37 °C at t = 0 and spindle formation monitored by immunofluorescence. No bipolar spindles formed in either strain and the rate of spindle formation in each medium was identical. *D*, Metabolism of arginine in *S. pombe.* For full description of genotype of mutant strains see methods section.

samples containing only medium-heavy amino acids arginine (Arg-6) and lysine (Lys-4), (Fig. 2*B*).

Ureases require Ni^{2+} as the major cofactor for their catalytic activity. *S. pombe* encodes one characterized urease (Ure1) (27) alongside several other proteins that are predicted to exercise urease activity. Nic1 is the sole plasma membrane Ni^{2+} transporter and supports urease activity of fission yeast (28). The observations of Eitinger *et al.* (28) led us to reason that the global reduction of the urease activity, arising from abolition of Nic1 function, would reduce the amino acid mislabeling we observed following growth of the *SILAC* strain on heavy arginine (Arg-10). We therefore deleted *nic1*$^+$ in the *SILAC* strain to generate "*SILACn*," before repeating the SILAC labeling as described above. As reported previously, *nic1*$^+$ ablation had no major impact upon the growth rate of otherwise wild type strains (Fig. 1*B*). Most importantly, the growth rate of *SILAC* and *SILACn* strains were identical (Fig. 1*B*), indicating that removal of *nic1*$^+$ is no more detrimental to cell physiology than the established mutations that are currently exploited for SILAC labeling in fission yeast (5).

Introduction of *nic1.*Δ increased the identification of arginine (Arg-10)-labeled peptides, suggesting that urease-dependent arginine catabolism was indeed a key factor in arginine (Arg-10) mislabeling (supplemental Fig. S1). However, the number of peptides that could be identified in samples labeled with heavy amino acids was below that obtained in samples containing light amino acids. Furthermore, the isotopic distribution of peptides was unusual, suggesting a partial incorporation of ^{15}N atoms. This incomplete suppression suggested either, that residual traces of Ni^{2+} persist in *nic1.*Δ cells, or that the urea is catabolized to ammonium ions by Ni^{2+} independent urease/pathways.

The increased identification rate of (Arg-10) labeled peptides in the *SILACn* background indicated that, although ^{15}N-ammonium has not been completely eliminated by removal of Nic1, its levels had been severely reduced. We therefore asked whether we could out compete the ability of the cells to incorporate these low levels of ^{15}N-ammonium ions in amino acid anabolic pathways, by supplementing the EMMG growth medium with levels of unlabeled ^{14}N-ammonium ions that are tolerated by *SILAC* strains (5). The *SILACn* strain grew with a doubling time of 5.5 h in EMMG media that contained 12 mM NH_4Cl (EMMGn) supplemented with standard "light" forms of both lysine and arginine. This doubling rate is close to the 5 h of the *SILAC* strain and 4.5 h of wild type prototrophs in the same medium. When stable isotope-labeled amino acids were used as the sole source of lysine and arginine the mid-log phase, the doubling rate increased to 7 h at 25 °C. For reasons that are not clear, the original *SILAC* strain (*nic1*$^+$) grew very poorly in EMMGn (supplemental Fig. S2). Impor-

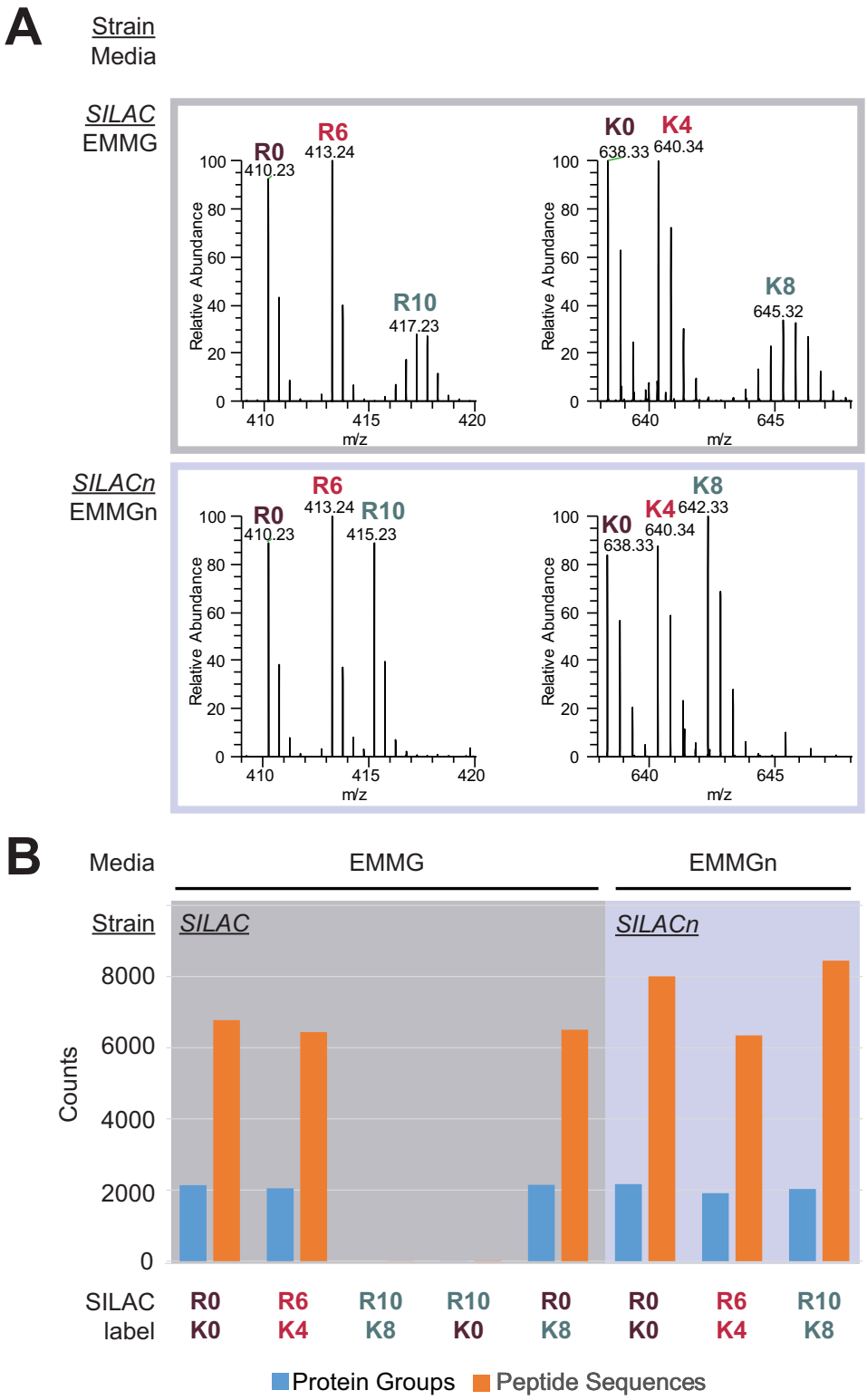

FIG. 2. **Assessment of arginine conversion using MS.** *A*, Isotopic distribution of peptides from a triple-SILAC experiment for an arginine and a lysine containing peptide using the *SILAC* strain (top) and an arginine and a lysine containing peptide using the *SILACn* strain (bottom). *B*, Protein groups (blue bars) and peptide sequences (orange bars) identified in individual experiments using different isotopic versions of lysine and arginine. The lines on the top indicate the media used and the colored background indicates the strain used.

TABLE I
Overview of the cdc25.22 arrest-release datasets

	K0 R0	K4 R8	K6 R10	Proteins Identified	Proteins Quantified (H/L)	Proteins Quantified (M/L)
Replicate 1	G2	M	G1S	3446	2672	2672
Replicate 2	M	G1S	G2	3462	2833	2833

Yeast strains

Strain No.	Genotype	Source
IH 1540	*h*$^+$ *lys1.131*	Lab Stock
IH 5224	*h*$^+$ *pku70::kanMX6 ura4.d18 leu1.32 ade6.704*	Lab Stock
IH 6113	*pku80::ura4*$^+$ *ura4.d18 leu1.32*	Lab Stock
IH 6297	*h*$^-$ *arg3.D4*	Lab Stock
IH 8987	*h*$^-$ *car2::NatMX6*	This study
IH 8988	*h*$^+$ *car2::NatMX6*	This study
IH 9091	*h*$^-$ *car2::NatMX6 lys1.131 arg3.D4 ura4.d18 leu1.32*	This study
IH 9092	*h*$^+$ *car2::NatMX6 lys1.131 arg3.D4 ura4.d18 leu1.32*	This study
IH 9281	*plo1.ts41:ura4*$^+$ *cut7.24 lys1.131 arg3.D4 car2::NatMX6 ura4.d18 leu1.32*	This study
IH 8439	*cut7.24 ura4.d18*	This study
IH 11849	*h*$^-$ *nic1::kanMX6 car2::NatMX6 lys1.131 arg3.D4*	This study
IH 13324	*cut7.24 nic1::kanMX6 car2::HphX6 arg3.D4 lys1-131*	This study
IH 13302	*cdc25.22 nic1::kanMX6 car2::HphX6 arg3.D4 lys1-131*	This study
IH 13303	*cdc10.v50 nic1::kanMX6 car2::HphX6 arg3.D4 lys1-131*	This study

tantly, however, the regular isotope pattern of the heavy-labeled peaks established that growth of *SILACn* cells in EMMGn successfully resolved the mislabeling problem (compare Fig. 2*A* top spectra with bottom spectra). This improved detection rate enabled us to identify comparable numbers of heavy labeled peptides to those that are routinely detected in cells labeled with light or medium amino acids (Fig. 2*B*).

Fission yeast is widely exploited for analysis of the cell division cycle. We therefore asked whether the combination of the *SILACn* background and EMMGn medium would impact upon the ability to use some well characterized mutations to synchronize progression through the cell division cycle. Removal of the function of the START transcription factor Cdc10 through the *cdc10.v50* mutation reversibly arrests cell cycle progression in G1, because cells are unable to transcribe genes encoding DNA replication factors (29). As S phase is initiated immediately after anaphase chromosome segregation, the vast majority of cells in an asynchronous *cdc10.v50* culture complete cytokinesis before accumulating at the G1 execution point (30). Transient cell cycle arrest at the *cdc10.v50* execution point is therefore a commonly employed approach to synchronize progression through S phase, immediately after the block to Cdc10 function that is triggered by the return to the permissive temperature. We asked whether this *cdc10.v50* "arrest release" approach could be used to synchronize S phase progression in a *SILACn background.* An early log phase *cdc10.v50 SILACn* culture was shifted to 36 °C before returning to 25 °C. FACs profiles indicated a proficient accumulation of 1N cells and an equally proficient reappearance of 2N cells following return to 25 °C. (supplemental Fig. S3*A*). Temperature dependent inactivation of Kinesin 5 through temperature shift of the *cut7.24* mutation removes the ability of the two half spindles to interdigitate. Consequently, the bipolar chromosome attachments that are required to silence the spindle assembly checkpoint (SAC) surveillance system are not established. This results in a persistent activation of the spindle assembly checkpoint that blocks cell cycle progression and so causes cells to accumulate in mitosis with monopolar spindles (26). The *cut7.24* mutation completely blocked spindle formation in EMMGn, irrespective of the presence of the *SILACn* mutations (supplemental Fig. S3*B*). Finally, we tested the combined impact of the *SILACn* mutations and growth in EMMGn upon the widely exploited ability of the *cdc25.22* mutation to reversibly arrest cell cycle progression at the G2/M boundary. Such *cdc25.22* "arrest release" cultures are highly synchronized with respect to mitotic progression (5, 21). *cdc25.22 SILACn* cells were grown to early log phase (1×10^6) in EMMGn at 25 °C before a transient shift to 36 °C for 4.25 h. The absence of the septa that identify cells undergoing cytokinesis indicated an efficient cell cycle arrest at the G2/M boundary (data not shown). The transient appearance of replication and 4n peaks in FACS analysis of DNA content 90–150 min after return to the permissive temperature of 25 °C indicated an equally efficient return to cycle after release (supplemental Fig. S4). We conclude that neither the inclusion of the *SILACn* mutations nor growth in EMMGn has a deleterious impact upon the ability to manipulate cell cycle progression to generate populations at discrete cell cycle or mitotic stages with the *cut7.24*, *cdc10.v50*, or *cdc25.22* mutations. The slightly slower growth rate of *SILACn* strains compared with WT is common among yeast auxotrophs. This reduced growth rate will have no major impact upon the interpretation of triple SILACn experiments because all three strains under query will harbor the same *SILACn* genetic background.

To validate this approach we performed a proof-of-principle triplex-SILAC measurement based on the duplex-SILAC *cdc25.22* arrest release experiment performed by Bicho *et al.*

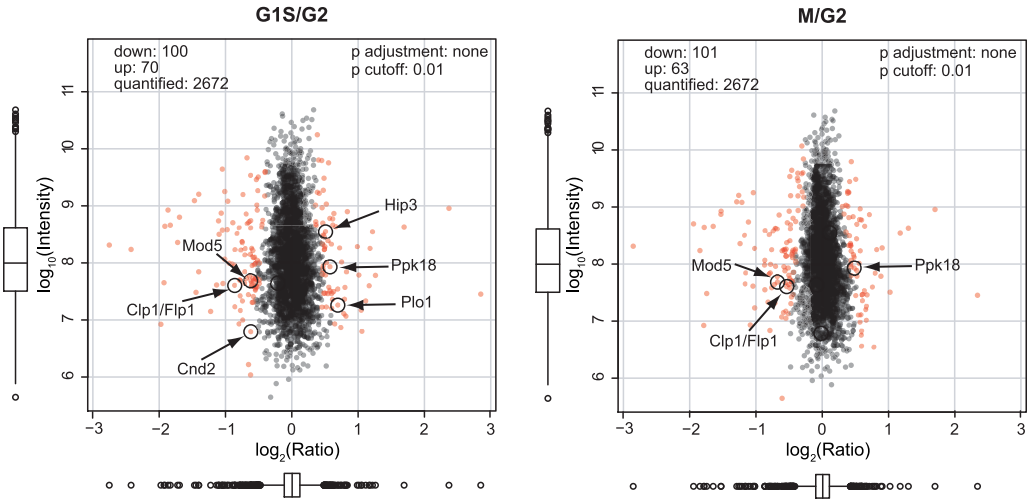

FIG. 3. **The proteome of cell cycle populations generated by the *cdc25. 22* arrest-release approach.** Log_2 transformed SILAC ratios of protein groups plotted against their respective log_{10} transformed intensity. On the left a comparison between G1S and G2 while a comparison between M and G2 is on the right. Significantly regulated proteins are marked in red; proteins discussed in the text are circled.

(5). In this experiment, we grew *cdc25.22 SILACn* cells in either EMMGn supplemented with arginine and lysine for "light," "medium-heavy," or "heavy" labeling. Cells were transiently arrested at the G2/M boundary before return to 25 °C, to release the arrest. FACs analysis revealed equivalent efficiencies of cell cycle progression following release in all cultures. Because the inclusion of the *nic1*.Δ mutation had generated the option of conducting triple-SILAC labeling, we supplemented the sampling at G2 and G1/S, performed by Bicho *et al.*, with a third time point in M phase (see Supplemental Fig. S4 for the time at which each sample was taken). In the first experiment, samples were labeled as follows: G2 (Lys-0, Arg-0), M (Lys-4, Arg-6), and G1S (Lys-8, Arg-10), in the second experiment we did a label swap: M (Lys-0, Arg-0), G1S (Lys-4, Arg-6), and G2 (Lys-8, Arg-10). An overview of the experiment can be found in Table I.

In 24 LC-MS runs, we recorded 747,658 MS/MS spectra that identified a total of 25,548 nonredundant peptides from 3606 *S. pombe* proteins, at estimated false discovery rate (FDR) of 1.30% at the protein level (supplemental Table S14). As shown in Table I, the use of Arg-10 did not influence peptide identification and the number of quantified M/L and H/L pairs were very similar, demonstrating that Arg-10 can be routinely used in SILAC measurements in the *cdc25.22 SILACn* strain. Of the 3075 quantified proteins, 2430 (79%) were quantified in both replicates and correlation was high ($R^2 = 0.89$), in spite of the fact that the labels were inversed in replicate analyses (supplemental Fig. S5*A*, 5*B*). We next compared our dataset to the data published by Bicho *et al.* (5) and observed good correlation ($R^2 = 0.59$) between proteins that were significantly regulated in both datasets. Importantly, this correlation was confirmed in the replicate measurement with inverted SILAC labels (Supplemental Fig. S5*C*, 5*D*). Thus, Arg-6 and Arg-10 labeling was robust. Despite a relative paucity of significantly regulated proteins in both datasets, we could confirm several findings observed by Bicho *et al.* (5, 31). In addition to several differentially regulated metabolic enzymes, we confirmed significant changes in the levels of polo kinase Plo1, condensin subunit Cnd2, and the HIRA histone chaperone complex hip3 in comparisons between the G2/G1+S datasets. We also detected significant regulation of the Cdc14 related cell cycle phosphatase Clp1/Flp1, the membrane anchor for the Tea1 cell morphogenesis complex, Mod5, and the Greatwall kinase family member Ppk18, in both the M/G2 and G2/G1+S datasets (Fig. 3).

We conclude that removal of Nic1 from cells grown in EMMGn finally renders fission yeast fully compatible with SILAC labeling, to greatly expand the options for interrogation of the *S. pombe* proteome. The ability to routinely conduct triple SILAC analysis in this genetically malleable model organism will rapidly advance our quantitative understanding of many core principles of molecular cell biology.

Acknowledgments—We thank M. Mann and S. Hauf for helpful comments on the manuscript, as well as K. Krug and C. Täumer for help with preparation of figures. We thank K. Gull (Oxford University) for TAT1 antibody.

* Our work is supported by funding from the Juniorprofessoren-Programm of the BW-Stiftung, FP7 PRIME-XS Consortium and SFB 766 of the German Research Council (DFG) to B.M. and by Cancer Research UK [CRUK] C147/A6058 to I.H., A.P., and Y.D.T.; A.P. was also supported by an EMBO STF.

[S] This article contains supplemental TablesS1 to S15 and Figs. S1 to S5.

Accession codes: The mass spectrometry data from this publication have been submitted to PeptideAtlas (www.peptideatlas.org) and assigned the accession number PASS00437. The fission yeast strain *h- nic1::kanMX6 arg3-D4 lys1-131 car2::NatMX6* has been submitted to Yeast Genetic Resource Center (http://yeast.lab.nig.ac.jp) and assigned accession number FY24007.

‖ To whom correspondence should be addressed: Proteome Center Tuebingen, Interfaculty Institute for Cell Biology, University of Tuebin-

gen, Auf der Morgenstelle 15, 72076 Tuebingen, Germany. Tel.: +49/7071/29-70558; Fax: +49/7071/29-5779; E-Mail: boris.macek@uni-tuebingen.de.

¶ These authors contributed equally to this work.

REFERENCES

1. Ong, S. E., and Mann, M. (2005) Mass spectrometry-based proteomics turns quantitative. *Nat. Chem. Biol.* **1,** 252–262
2. Ong, S. E., Blagoev, B., Kratchmarova, I., Kristensen, D. B., Steen, H., Pandey, A., and Mann, M. (2002) Stable isotope labeling by amino acids in cell culture, SILAC, as a simple and accurate approach to expression proteomics. *Mol. Cell. Proteomics* **1,** 376–386
3. Olsen, J. V., Blagoev, B., Gnad, F., Macek, B., Kumar, C., Mortensen, P., and Mann, M. (2006) Global, in vivo, and site-specific phosphorylation dynamics in signaling networks. *Cell* **127,** 635–648
4. de Godoy, L. M. F., Olsen, J. V., de Souza, G. A., Li, G. Q., Mortensen, P., and Mann, M. (2006) Status of complete proteome analysis by mass spectrometry: SILAC labeled yeast as a model system. *Genome Biol.* **7,** R50
5. Bicho, C. C., Alves, F. D., Chen, Z. A., Rappsilber, J., and Sawin, K. E. (2010) A genetic engineering solution to the "arginine conversion problem" in Stable Isotope Labeling by Amino Acids in Cell Culture (SILAC). *Mol. Cell. Proteomics* **9,** 1567–1577
6. de Godoy, L. M., Olsen, J. V., Cox, J., Nielsen, M. L., Hubner, N. C., Frohlich, F., Walther, T. C., and Mann, M. (2008) Comprehensive mass-spectrometry-based proteome quantification of haploid versus diploid yeast. *Nature* **455,** 1251–1254
7. Elledge, S. J. (1996) Cell cycle checkpoints: preventing an identity crisis. *Science* **274,** 1664–1672
8. White, S. A., and Allshire, R. C. (2008) RNAi-mediated chromatin silencing in fission yeast. *Curr. Top. Microbiol.* **320,** 157–183
9. Harigaya, Y., and Yamamoto, M. (2007) Molecular mechanisms underlying the mitosis–meiosis decision. *Chromosome Res.* **15,** 523–537
10. Marguerat, S., Schmidt, A., Codlin, S., Chen, W., Aebersold, R., and Bahler, J. (2012) Quantitative analysis of fission yeast transcriptomes and proteomes in proliferating and quiescent cells. *Cell* **151,** 671–683
11. Gunaratne, J., Schmidt, A., Quandt, A., Neo, S. P., Sarac, O. S., Gracia, T., Loguercio, S., Ahrne, E., Xia, R. L., Tan, K. H., Lossner, C., Bahler, J., Beyer, A., Blackstock, W., and Aebersold, R. (2013) Extensive mass spectrometry-based analysis of the fission yeast proteome: the *Schizosaccharomyces pombe* PeptideAtlas. *Mol. Cell. Proteomics* **12,** 1741–1751
12. Koch, A., Krug, K., Pengelley, S., Macek, B., and Hauf, S. (2011) Mitotic substrates of the kinase aurora with roles in chromatin regulation identified through quantitative phosphoproteomics of fission yeast. *Sci. Signal.* **4,** rs6
13. Moreno, S., Klar, A., and Nurse, P. (1991) Molecular genetic analysis of fission yeast *Schizosaccharomyces pombe*. *Methods Enzymol.* **194,** 795–823
14. Fantes, P., and Nurse, P. (1977) Control of cell size at division in fission yeast by a growth-modulated size control over nuclear division. *Exp. Cell Res.* **107,** 377–386
15. Nurse, P. (1975) Genetic control of cell size at cell division in yeast. *Nature* **256,** 547–551
16. Hentges, P., Van Driessche, B., Tafforeau, L., Vandenhaute, J., and Carr, A. M. (2005) Three novel antibiotic marker cassettes for gene disruption and marker switching in *Schizosaccharomyces pombe*. *Yeast* **22,** 1013–1019
17. Krug, K., Carpy, A., Behrends, G., Matic, K., Soares, N. C., and Macek, B. (2013) Deep coverage of the *Escherichia coli* proteome enables the assessment of false discovery rates in simple proteogenomic experiments. *Mol. Cell. Proteomics* **12,** 3420–3430
18. Rappsilber, J., Mann, M., and Ishihama, Y. (2007) Protocol for micro-purification, enrichment, prefractionation, and storage of peptides for proteomics using StageTips. *Nat. Protoc.* **2,** 1896–1906
19. Cox, J., and Mann, M. (2008) MaxQuant enables high peptide identification rates, individualized p.p.b.-range mass accuracies, and proteome-wide protein quantification. *Nat. Biotechnol.* **26,** 1367–1372
20. Cox, J., Neuhauser, N., Michalski, A., Scheltema, R. A., Olsen, J. V., and Mann, M. (2011) Andromeda: a peptide search engine integrated into the maxquant environment. *J. Proteome Res.* **10,** 1794–1805
21. Tay, Y. D., Patel, A., Kaemena, D. F., and Hagan, I. M. (2013) Mutation of a conserved residue enhances the sensitivity of analog-sensitized kinases to generate a novel approach to the study of mitosis in fission yeast. *J. Cell Sci.* **126,** 5052–5061
22. Woods, A., Sherwin, T., Sasse, R., MacRae, T. H., Baines, A. J., and Gull, K. (1989) Definition of individual components within the cytoskeleton of *Trypanosoma brucei* by a library of monoclonal antibodies. *J. Cell Sci.* **93,** 491–500
23. Fantes, P. A., and Creanor, J. (1984) Canavanine resistance and the mechanism of arginine uptake in the fission yeast *Schizosaccharomyces pombe*. *J. Gen. Microbiol.* **130,** 3265–3273
24. Petersen, J. (2009) TOR signaling regulates mitotic commitment through stress-activated MAPK and Polo kinase in response to nutrient stress. *Biochem. Soc. T.* **37,** 273–277
25. Grallert, A., Patel, A., Tallada, V. A., Chan, K. Y., Bagley, S., Krapp, A., Simanis, V., and Hagan, I. M. (2013) Centrosomal MPF triggers the mitotic and morphogenetic switches of fission yeast. *Nat. Cell Biol.* **15,** 88–95
26. Hagan, I., and Yanagida, M. (1990) Novel potential mitotic motor protein encoded by the fission yeast cut7+ gene. *Nature* **347,** 563–566
27. Lubbers, M. W., Rodriguez, S. B., Honey, N. K., and Thornton, R. J. (1996) Purification and characterization of urease from *Schizosaccharomyces pombe*. *Can. J. Microbiol.* **42,** 132–140
28. Eitinger, T., Degen, O., Bohnke, U., and Muller, M. (2000) Nic1p, a relative of bacterial transition metal permeases in *Schizosaccharomyces pombe*, provides nickel ion for urease biosynthesis. *J. Biol. Chem.* **275,** 18029–18033
29. Marks, J., Fankhauser, C., Reymond, A., and Simanis, V. (1992) Cytoskeletal and DNA structure abnormalities result from bypass of requirement for the cdc10 start gene in the fission yeast *Schizosaccharomyces pombe*. *J. Cell Sci.* **101,** 517–528
30. Nurse, P., Thuriaux, P., and Nasmyth, K. (1976) Genetic control of the cell division cycle in the fission yeast *Schizosaccharomyces pombe*. *Mol. Gen. Genet.* **146,** 167–178
31. Carpy, A., Krug, K., Graf, S., Koch, A., Popic, S., Hauf, S., and Macek, B. (2014) Absolute proteome and phosphoproteome dynamics during the cell cycle of fission yeast. *Mol. Cell. Proteomics* **13,** 1925–1936